Detection of single gold nanoparticles using spatial modulation spectroscopy implemented with a galvo-scanning mirror system

Mary Sajini Devadas, Zhongming Li, Todd A. Major, Shun Shang Lo, Nicolas Havard, Kuai Yu, Paul Johns, and Gregory V. Hartland*

Department of Chemistry and Biochemistry, University of Notre Dame, Notre Dame, Indiana 46556-5670, USA *Corresponding author: ghartlan@nd.edu

Received 12 August 2013; revised 16 October 2013; accepted 17 October 2013; posted 18 October 2013 (Doc. ID 195508); published 8 November 2013

The optical extinction of single nanoparticles can be sensitively detected by spatial modulation spectroscopy (SMS), where the particle is moved in and out of a tightly focused laser beam with a piezo-device. Here we show that high sensitivity can be obtained by modulating the beam with a galvo-mirror system, rather than by moving the sample. This work demonstrates an inexpensive method for making a SMS microscope, and shows how an existing laser scanning microscope can be adapted for SMS measurements. The galvo-mirror technique also allows SMS measurements to be performed in a liquid, which is difficult to do with piezo-modulation. © 2013 Optical Society of America

Optical detection of single nano-objects with low fluorescence quantum yields is challenging. Recently. several absorption-based techniques have been developed that can be used to study particles with sizes of a few nanometers [1-6]. One widely used method is photothermal heterodyne imaging (PHI), where a nonresonant probe is used to detect the heat deposited into the sample by a modulated pump beam [1-3,7,8]. PHI has sufficient sensitivity to detect single molecules [3] and can also be used to study particles freely diffusing in a liquid [9,10]. However, PHI does not give direct information about the extinction cross section of the nano-object being interrogated [11,12], which is extremely useful for characterization. In this regard, an attractive technique for studying small particles is spatial modulation spectroscopy (SMS) [13–16]. In SMS the particle is moved in and out of the laser focal spot, and the

change in transmitted power is recorded using a lock-in amplifier. These measurements directly yield the extinction cross section, which can be compared to theory to determine the size of the particle [14,16].

In the standard implementation of SMS, a piezo-device is used to laterally modulate the sample position by a few hundred nanometers at kilohertz frequencies [13–16]. In terms of sensitivity, single 5 nm nanoparticles can be detected with a signalto-noise ratio comparable to PHI [13]. SMS has also been used to record the spectra of single metallic and semiconductor nanostructures [14-17], which is difficult to do with PHI [18]. However, an obvious drawback to SMS is that it is a low-frequency technique, which limits the sensitivity (due to 1/f noise), as well as the speed at which data can be collected. Several recent papers have addressed these issues. Fairbairn et al. improved the acquisition time of SMS by using a piezo-activated flexure mirror to modulate the position of a beam focused to a line at the sample, in conjunction with a line camera [19]. They demonstrated signal-to-noise

1559-128X/13/327806-06\$15.00/0 © 2013 Optical Society of America levels greater than 100 for 200 nm diameter gold particles at video rates. Recently, Oudjedi *et al.* used an acousto-optic deflector (AOD) to achieve modulation frequencies of 100 kHz [20]. They were able to measure the extinction cross sections of 10 nm gold spheres with signal-to-noise of >20 for a 25 ms integration time, as well as to detect isolated single wall carbon nanotubes.

In this paper we describe the use of galvo-scanning mirrors (GSMs, Thorlabs, GVSM0002) to modulate the beam at the sample, rather than the sample at the beam. Figure 1 gives a schematic of the experimental setup. The reference output from a lock-in amplifier (Stanford Research Instruments, SR830) was used to wobble the GSMs, and the voltage applied to the GSM system was adjusted to give a modulation amplitude of 0.2 µm at the sample. The deflection of the laser beam at the sample was determined by calibrating the response of the GSM with a ruled microscope slide. The beam from a 532 nm CW laser (Spectra Physics, Millennia Vs) was directed through the GSM system, and then sent to an inverted optical microscope (Olympus, IX71) using a 4f lens system, where it was focused at the sample with a high numerical aperture (NA) objective (Olympus UPlan FLN, 100X 1.3 NA). A second high NA objective recollimates the beam, which is then directed to a Si photodiode detector (PD) by a second 4f lens system. The 4f lens systems project the beam from the GSM to the back aperture of the focusing objective, and from the back aperture of the collimation objective to the detector. This is necessary to avoid clipping the beam as it is scanned over the sample. The DC component of the PD signal was recorded with a digital voltmeter (Keithley, 2000) Multimeter), and the in-phase (X) component of the modulated signal was recorded by the lock-in amplifier. Careful alignment of the lens systems reduces the background in the SMS experiments to $\Delta I/I$ < 10⁻⁵ (without the sample), which is similar to the background levels in SMS experiments implemented with piezo-stage modulation.

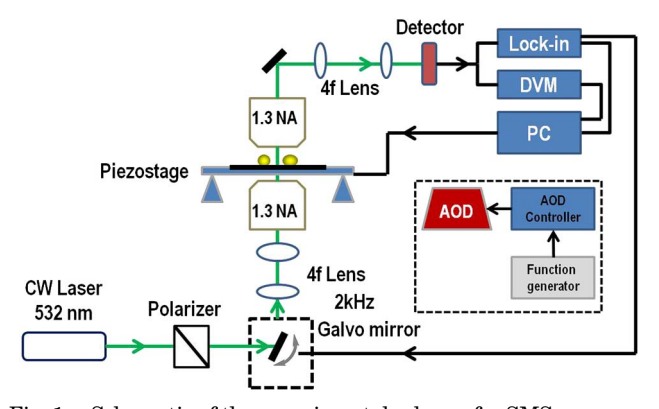


Fig. 1. Schematic of the experimental scheme for SMS measurements with a galvo-scanning mirror system. The inset shows the setup with the AOD. DVM, digital voltmeter; AOD, acousto-optic deflector.

SMS images were generated by raster scanning the sample through the laser spot using a piezo-stage (Physik Instrumente, P-527. 3Cl), or by scanning the beams over the sample with the GSMs. Typically a lock-in time constant of 10 ms was used, with a 30 ms pixel dwell time for imaging. Since this system involves the deflection of the beam rather than movement of the stage, it can (in principle) be performed at a higher frequency. However, for our experiments the frequency is currently limited to 2 kHz, due to the feedback loop in the GSM drive electronics. Note that this optical system is similar to the one reported by Oudjedi et al. for SMS implemented with an AOD [20]. As part of this work we compare the performance of the GSM system to an AOD (IntraAction Corp.); however, the majority of the experiments were performed with the GSMs.

The samples in these experiments were synthesized using standard wet chemical methods [21]. Briefly, 750 µL of a 1% by weight sodium citrate solution was added to 50 mL of a boiling solution of 0.01% HAuCl₄ · 3H₂O in water. The solution turned black at first, followed by the formation of a ruby red solution. The mixture was refluxed for another 10 min, and then cooled to room temperature. The particles had an average size of 23 ± 2 nm (error equals standard deviation), as measured by transmission electron microscopy (TEM, JEOL 2010). Gold nanoparticle samples with sizes of 35 ± 4 nm and 51 ± 3 nm were also prepared by using 300 and 200 µL of the sodium citrate solution, respectively. A gold nanoparticle sample with a nominal size of 10 nm was purchased from BBI. Subsequent TEM analysis of this sample shows a size distribution of 9 ± 1 nm. Samples for SMS imaging experiments were prepared by spin coating a dilute solution of the nanoparticles onto a glass coverslip. For the correlation measurements described below, a drop of nanoparticle solution was added to a coverslip, and the focus of the laser was adjusted to be a few tens of micrometers above the surface of the coverslip, within the volume of the solution.

For a nanoparticle with dimensions much smaller than the wavelength of the light, the transmitted power P_t of a laser beam impinging on the particle is given by $P_t = P_i - \sigma_{\rm ext} I(x,y)$, where P_i is the incident power, I(x,y) is the intensity of the beam at the position of the particle, and $\sigma_{\rm ext}$ is the extinction cross section [13–16]. For a small modulation in either the particle or beam position (for example, $y \to y + \delta \sin(2\pi ft)$) the transmitted power can be Taylor expanded into a Fourier series in the modulation frequency, where the coefficients for the different frequency terms involve $\sigma_{\rm ext}$, the spot size of the laser beam, the degree of modulation δ , and the first, second, third, etc., derivatives of I(x,y). These different terms can be separately measured by the lock-in amplifier.

Figures $\underline{2A}$ – $\underline{2D}$ show SMS results obtained from a Au nanoparticle sample with an average diameter of 23 ± 2 nm, using the GSM system for beam

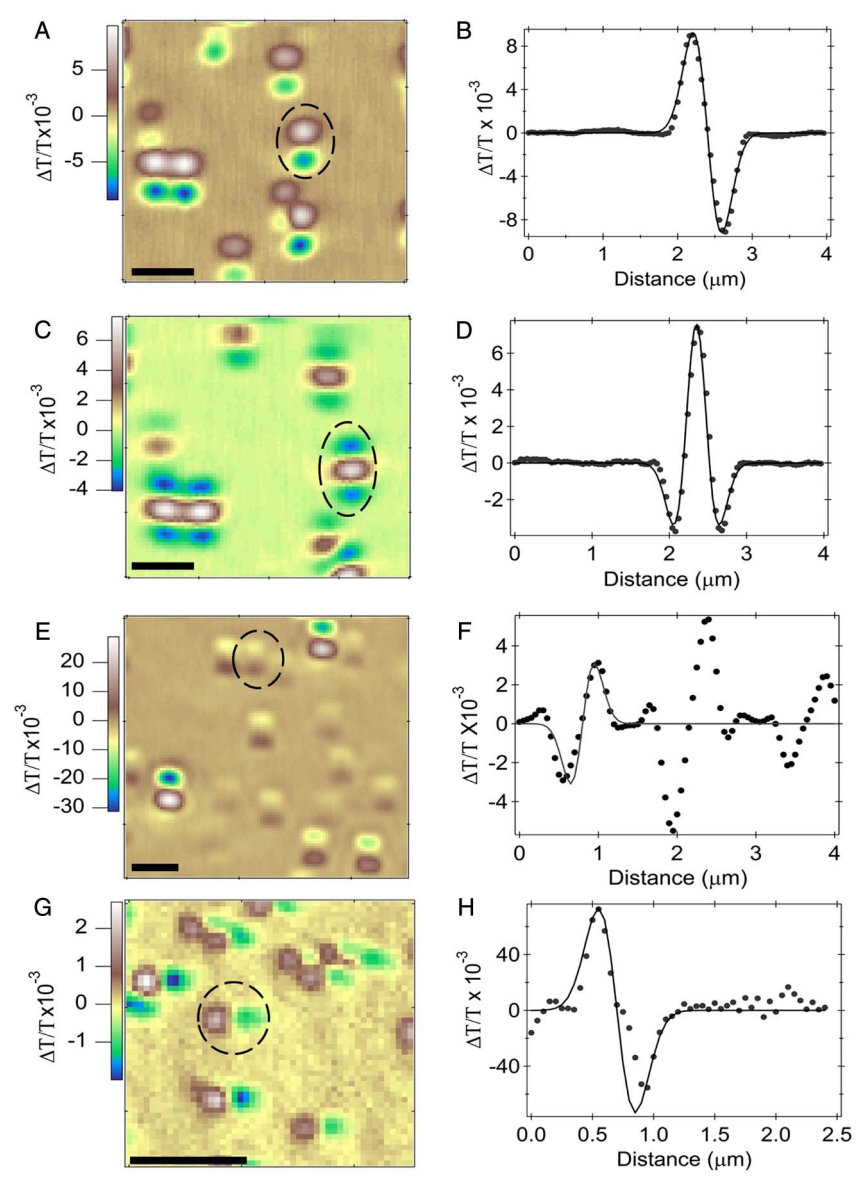


Fig. 2. A, 1f contour plot of the 23 \pm 2 nm sample; B, line profile of a particle in A along with a fit to the data; C, 2f contour plot of the same area as in A; D, line profile for the same particle as in B. The data were recorded with a lock-in time constant of 10 ms, a 30 ms pixel dwell time, and an incident laser power of 100 μ W. E, 1f contour plot of the 9 \pm 1 nm sample; F, line plot of a particle with a fit; G, 1f contour plot of the 23 \pm 2 nm sample using an AOD; H, corresponding line profile and fit for a particle. The scale bar in all the images is 1 μ m. The circles indicate the particles analyzed in the line profiles.

modulation. Figures $\underline{2A}$ and $\underline{2C}$ are contour plots of a 4 μ m × 4 μ m area recorded at the fundamental f and second-harmonic 2f frequencies. The data at f and 2f have the characteristic lineshapes expected for the first and second derivatives of a Gaussian beam $[\underline{13},\underline{14}]$. Figures $\underline{2B}$ and $\underline{2D}$ show line profiles of the data in Figs. $\underline{2A}$ and $\underline{2C}$, along with fits to the data using the expressions given in Refs. $[\underline{13}-\underline{16}]$. In these fits the beam size and $\sigma_{\rm ext}$ were used as fitting parameters. We obtain $\sigma_{\rm ext}=380\pm30~{\rm nm}^2$ for the particle in Figs. $\underline{2B}$ and $\underline{2D}$, with a spot size of $w_0=380\pm15~{\rm nm}$ (this value was determined by fitting the response from a number of particles).

The signal-to-noise level for the data in Figs. $\underline{2A}$ and $\underline{2B}$ is approximately 90:1. Figures $\underline{2E}$ and $\underline{2F}$

show analogous contour plots (5 $\mu m \times 5~\mu m$ area) and line profiles for a Au nanoparticle sample with an average size of 9 \pm 1 nm (error equals standard deviation). The signal-to-noise for this data is approximately 20:1, which is comparable to the signal-to-noise levels obtained for SMS experiments where the sample position is modulated. The signal-to-noise in these measurements depends on inhomogeneities in the substrate, which can cause a background signal in SMS experiments. Improvements in the signal-to-noise could be achieved by using microscope oil to index match with the glass slide.

The data in Figs. 2A and 2C show different signal levels for different particles, which is due to

differences in particle size. The average cross sections measured for the two samples in Figs. 2A-2F are $340\pm108~\text{nm}^2$ and $40\pm15~\text{nm}^2$ (error equals standard deviation, approximately 40 particles interrogated for each sample). The measured cross sections can be converted to particle size by comparison with Mie theory calculations [13,22]. In these calculations the effective dielectric constant of the medium was set to the average value of glass and air [22,23]. We obtain particle diameters of $20\pm5~\text{nm}$ and $11\pm3~\text{nm}$, respectively, which are in reasonable agreement with the average sizes determined by TEM analysis of the samples.

In an attempt to improve the signal-to-noise ratio in these experiments, we used an AOD to modulate the beam position at a higher frequency [20]. The AOD allows us to achieve modulation frequencies of up to 500 kHz; however, the best images were obtained at 50 kHz. In these experiments the firstorder diffracted beam from the AOD was directed through the 4f lens system to the microscope. The diffraction angle was then changed by changing the frequency of the acoustic wave in the AOD. This was achieved by applying a modulated voltage to the frequency control of the AOD drive electronics. However, because the diffraction efficiency of the AOD has a Bragg condition, we found it very difficult to keep the intensity of the beam constant as it was moved at the sample. Specifically, the Bragg angle for the deflector is $\theta_B \approx F \lambda/v$, where *F* is the acoustic frequency, λ is the wavelength of light, and v is the velocity of sound in the AOD. Changes in F change θ_B , which changes the diffraction efficiency for a fixed alignment of the AOD. This creates a background in the SMS image, which degrades the signal-to-noise. Our best results were obtained using square-wave modulation of the drive frequency, which creates two spots at the sample, and adjusting the angle of the AOD to minimize the background signal (i.e., to equalize the intensity of the two spots). Figure 2G is a contour plot of the 23 ± 2 nm sample obtained using the AOD, and Fig. 2H is a line profile from the image. The signal-to-noise level is approximately 10:1, and is clearly worse than that obtained using the GSMs.

We have also used the GSM-SMS experiments to study particles in a liquid. Figure 3 shows SMS time traces for nanoparticles freely diffusing in water, and in a water-glycerol mixture. Two samples were examined, one with an average size of 35 ± 4 nm (Fig. 3A) and another with an average size of 51 ± 3 nm (Figs. 3B and 3C). The smaller particles clearly show faster diffusion, which is confirmed by correlation analysis of the data [9,10,24,25]. These measurements were conducted by recording the magnitude of the fundamental signal from the lock-in amplifier $(R = \sqrt{X^2 + Y^2})$, with a time constant of 3 ms and a 10 ms bin time. (Equivalent results were obtained at the second harmonic, but with worse signal-to-noise because of the lower signal level.) The bin time limits the short time response

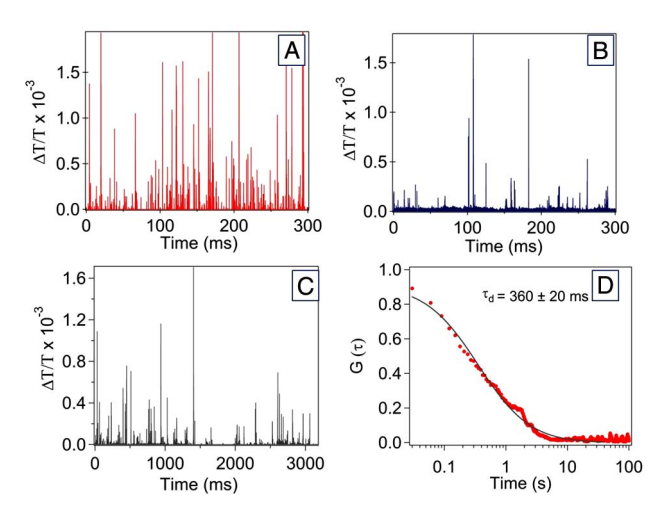


Fig. 3. A, time trace for diffusion of 35 ± 4 nm particles into the laser focal volume; B, time trace for 51 ± 3 nm particles. Both traces were recorded in water. The data were recorded with a lock-in time constant of 3 ms, 10 ms between points, and a laser power of 200 μW . C, time trace for the 51 ± 3 nm particles in a 30% H_2O –glycerol solution; D, corresponding correlation analysis of the data in C.

of the experiments, and means that the data in Figs. 3A and 3B cannot be accurately analyzed to yield a diffusion time [9,10,24,25]. We found that reducing the lock-in time constant to less than 3 ms (in order to reduce the bin time) leads to a significant increase in the noise for our 2 kHz modulation frequency. Measurements were also carried out in water-glycerol samples, which give slower diffusion times. A time trace for the 51 ± 3 nm particles in a 30% water-glycerol solution is shown in Fig. 3C, and the corresponding correlation analysis is shown in Fig. 3D. A fit to the correlation data using the formula for three-dimensional diffusion is also presented in Fig. 3D [24]. This fit yields a diffusion time of 360 ± 20 ms, which is consistent with previous correlation measurements of gold particles diffusing in water-glycerol solutions obtained using PHI [10]. Note that in principle, these experiments could be performed by modulating the sample position with a piezo-stage, as demonstrated by single particle tracking experiments [26,27]. However, the modulation frequency would be much lower in this case, further increasing the bin time.

Finally, the GSM system can also be used to scan the beam over the sample, as well as modulate the beam position. In these experiments a DC voltage generated by the computer is added to the AC signal from the lock-in reference with a simple voltage adder. The DC voltage controls the overall angle of the beam from the GSM system and, therefore, the position of the beam at the sample (as in a regular laser scanning confocal microscope system), and the AC voltage provides a small modulation of the beam position along the x or y axis. SMS data for the 51 ± 3 nm gold nanoparticle sample recorded in transmission mode with the GSMs being used to scan the beam are presented in Fig. 4A. Figure 4B

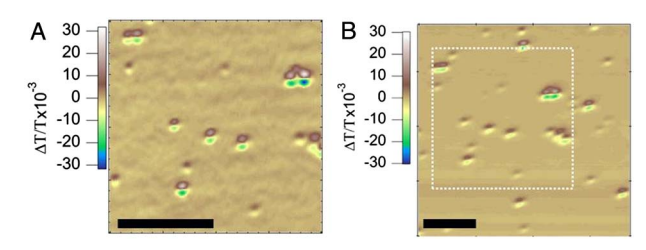


Fig. 4. A, 1f contour plot of the 51 \pm 3 nm sample using the GSM system; B, 1f contour plot of the same area obtained by moving the piezo-stage. The data were recorded with a lock-in time constant of 10 ms, a 30 ms pixel dwell time, 0.1 μm step size, and an incident laser power of 200 μW . The scale bars correspond to 1 μm . Both images were obtained in transmission configuration.

shows data recorded over the same region where the piezo-stage was used to scan the sample position. The two images are essentially identical.

Note that the signal-to-noise is slightly worse in the beam-scanning experiment (Fig. 4A), due to the appearance of small "waves" in the background. We believe that these features arise from an etalon effect in a 90% beam splitter before the microscope objective (this optic is inside the inverted microscope and is not shown in the schematic diagram of Fig. 1). Specifically, the reflections from the two faces of the beam splitter interfere at the detector. When the GSM is used to scan the beam over the sample, the angle of the beams at the beam splitter changes. This causes small pathlength differences for the different reflections from the beam splitter, which cause etalon effects in the detected signal. Images recorded with the beam splitter turned around, so that the reflective face is at the back, give larger fringes, as expected for an etalon effect. We believe that this effect could be greatly reduced by using better optics in the measurements, or by constructing a homebuilt microscope for SMS measurements that does not have a beam splitter as part of the optics path.

In conclusion, this paper describes a modification of SMS where a galvo-mirror system is used to spatially modulate the beam at the sample. The technique is similar to the experiments recently reported by Oudjedi et al., in which an AOD is used for modulation [20]. The GSM approach offers several advantages compared to the AOD: first (in our hands) the signal-to-noise from the GSM system is better. This is due to a background signal from the AOD caused by changes in the diffraction efficiency as the beam position is modulated. Second, the GSM system is achromatic: the same degree of modulation occurs for different wavelengths, unlike for an AOD, where the amount of deflection at a given applied acoustic frequency is proportional to the wavelength. Finally, the GSM can also be used to scan the beam over the sample. This means that a SMS microscope can be constructed without a piezo-stage, resulting in a significant cost reduction. These results also show that SMS could be implemented on existing laser scanning confocal microscopes, with only a simple addition to the electronics for the GSM system.

However, a disadvantage of this technique is that it is still relatively low frequency; improvements in signal-to-noise could be achieved by increasing the modulation frequency.

This work was supported by the National Science Foundation (CHE-1110560) and the Office of Naval Research (Award No. N00014-12-1-1030). The authors acknowledge Felix Vietmeyer, Matthew McDonald, and Dr. Masaru Kuno for their help during the measurements.

References

- 1. S. P. Berciaud, L. Cognet, G. A. Blab, and B. Lounis, "Photothermal heterodyne imaging of individual nonfluorescent nanoclusters and nanocrystals," Phys. Rev. Lett. 93, 257402 (2004).
- A. Gaiduk, P. V. Ruijgrok, M. Yorulmaz, and M. Orrit, "Detection limits in photothermal microscopy," Chem. Sci. 1, 343–350 (2010).
- 3. A. Gaiduk, M. Yorulmaz, P. V. Ruijgrok, and M. Orrit, "Room-temperature detection of a single molecule's absorption by photothermal contrast," Science **330**, 353–356 (2010).
- P. Kukura, M. Celebrano, A. Renn, and V. Sandoghdar, "Single-molecule sensitivity in optical absorption at room temperature," J. Phys. Chem. Lett. 1, 3323–3327 (2010).
- M. Celebrano, P. Kukura, A. Renn, and V. Sandoghdar, "Single-molecule imaging by optical absorption," Nat. Photonics 5, 95–98 (2011).
- S. S. Chong, W. Min, and X. S. Xie, "Ground-state depletion microscopy: detection sensitivity of single-molecule optical absorption at room temperature," J. Phys. Chem. Lett. 1, 3316–3322 (2010).
- M. Selmke, M. Braun, and F. Cichos, "Photothermal singleparticle microscopy: detection of a nanolens," ACS Nano 6, 2741–2749 (2012).
- W. S. Chang and S. Link, "Enhancing the sensitivity of singleparticle photothermal imaging with thermotropic liquid crystals," J. Phys. Chem. Lett. 3, 1393–1399 (2012).
- R. Radunz, D. Rings, K. Kroy, and F. Cichos, "Hot Brownian particles and photothermal correlation spectroscopy," J. Phys. Chem. A 113, 1674–1677 (2009).
- P. M. R. Paulo, A. Gaiduk, F. Kulzer, S. F. G. Krens, H. P. Spaink, T. Schmidt, and M. Orrit, "Photothermal correlation spectroscopy of gold nanoparticles in solution," J. Phys. Chem. C 113, 11451–11457 (2009).
- M. Selmke, M. Braun, and F. Cichos, "Gaussian beam photothermal single particle microscopy," J. Opt. Soc. Am. A 29, 2237–2241 (2012).
- P. Berto, E. B. Urena, P. Bon, R. Quidant, H. Rigneault, and G. Baffou, "Quantitative absorption spectroscopy of nano-objects," Phys. Rev. B 86, 165417 (2012).
- A. Arbouet, D. Christofilos, N. Del Fatti, F. Vallée, J. R. Huntzinger, L. Arnaud, P. Billaud, and M. Broyer, "Direct measurement of the single-metal-cluster optical absorption," Phys. Rev. Lett. 93, 127401 (2004).
- V. Juvé, M. F. Cardinal, A. Lombardi, A. Crut, P. Maioli, J. Pérez-Juste, L. M. Liz-Marzán, N. Del Fatti, and F. Vallée, "Size-dependent surface plasmon resonance broadening in nonspherical nanoparticles: single gold nanorods," Nano Lett. 13, 2234–2240 (2013).
- P. Billaud, S. Marhaba, N. Grillet, E. Cottancin, C. Bonnet, J. Lerme, J. L. Vialle, M. Broyer, and M. Pellarin, "Absolute optical extinction measurements of single nano-objects by spatial modulation spectroscopy using a white lamp," Rev. Sci. Instrum. 81, 043101 (2010).
- A. Lombardi, M. Loumaigne, A. Crut, P. Maioli, N. Del Fatti,
 F. Vallée, M. Spuch-Calvar, J. Burgin, J. Majimel, and M. Treguer-Delapierre, "Surface plasmon resonance properties of single elongated nanoobjects: gold nanobjpyramids and nanorods," Langmuir 28, 9027–9033 (2012).

- J. Giblin, F. Vietmeyer, M. P. McDonald, and M. Kuno, "Single nanowire extinction spectroscopy," Nano Lett. 11, 3307–3311 (2011).
- S. Berciaud, L. Cognet, P. Tamarat, and B. Lounis, "Observation of intrinsic size effects in the optical response of individual gold nanoparticles," Nano Lett. 5, 515–518 (2005).
- N. Fairbairn, R. A. Light, R. Carter, R. Fernandes, A. G. Kanaras, T. J. Elliott, M. G. Somekh, M. C. Pitter, and O. L. Muskens, "Spatial modulation microscopy for real-time imaging of plasmonic nanoparticles and cells," Opt. Lett. 37, 3015–3017 (2012).
- L. Oudjedi, A. N. G. Parra-Vasquez, A. G. Godin, L. Cognet, and B. Lounis, "Metrological investigation of the (6,5) carbon nanotube absorption cross section," J. Phys. Chem. Lett. 4, 1460–1464 (2013).
- 21. G. Frens, "Controlled nucleation for regulation of the particle size in monodisperse gold suspensions," Nat. Phys. Sci. **241**, 20–22 (1973)
- 22. O. L. Muskens, N. Del Fatti, F. Vallée, J. R. Huntzinger, P. Billaud, and M. Broyer, "Single metal nanoparticle absorption spectroscopy and optical characterization," Appl. Phys. Lett. 88, 063109 (2006).

- 23. A. Curry, G. Nusz, A. Chilkoti, and A. Wax, "Substrate effect on refractive index dependence of plasmon resonance for individual silver nanoparticles observed using darkfield micro-spectroscopy" Opt. Express 13, 2668–2677 (2005).
- micro-spectroscopy," Opt. Express 13, 2668–2677 (2005).

 24. A. Tcherniak, S. Dominguez-Medina, W. S. Chang, P. Swanglap, L. S. Slaughter, C. F. Landes, and S. Link, "One-photon plasmon luminescence and its application to correlation spectroscopy as a probe for rotational and translational dynamics of gold nanorods," J. Phys. Chem. C 115, 15938–15949 (2011).
- M. Loumaigne, P. Vasanthakumar, A. Lombardi, A. Richard, and A. Debarre, "One-photon excited luminescence of single gold particles diffusing in solution under pulsed illumination," Phys. Chem. Chem. Phys. 15, 4154–4162 (2013)
- H. Cang, C. M. Wong, S. Xu, A. H. Rizvi, and H. Yang, "Confocal three dimensional tracking of a single nanoparticle with concurrent spectroscopic readouts," Appl. Phys. Lett. 88, 223901 (2006).
- C. S. Xu, H. Cang, D. Montiel, and H. Yang, "Rapid and quantitative sizing of nanoparticles using three-dimensional single-particle tracking," J. Phys. Chem. C 111, 32–35 (2007).